Kinetics of H atom adsorption on Si(100) at 500–650 K

A. Kutana, B. Makarenko,[a] and J. W. Rabalais[b]
Department of Chemistry, University of Houston, Houston, Texas 77204-5641

(Received 14 May 2003; accepted 16 September 2003)

The kinetics of isothermal adsorption and migration of atomic hydrogen on a Si(100) surface has been investigated by the time-of-flight scattering and recoiling spectrometry technique. A continuous decrease in saturation coverage with temperature under constant atomic hydrogen exposure has been observed for temperatures in the range 325–750 K. This observation is in contrast with a widely accepted view of the Si(100)/H surface as having three fixed coverage states within certain temperature windows. For $T_S = 500-650$ K, the decrease is described by a kinetic model in which the surface concentration of physisorbed hydrogen atoms is depleted due to the increased rate of migration from precursor sites to primary monohydride sites. The model suggests a mechanism to explain the dependence of the saturation value on temperature in this range. The migration constant obeys an Arrhenius expression with an activation energy of 0.71 eV. A significant concentration of hydrogen atoms occupying precursor states acts as a reservoir, saturating the monohydride dangling bonds after the hydrogen source is shut off and discontinuation of Eley–Rideal abstraction. © *2003 American Institute of Physics.* [DOI: 10.1063/1.1624827]

I. INTRODUCTION

The adsorption and desorption of hydrogen from the Si(100) surface has received much attention in recent years.[1–21] From a technological viewpoint, the presence of hydrogen in the gas phase and as a surfactant plays an important role in crystal growth on silicon substrates. Examples of how hydrogen affects epitaxial growth processes are an increase in island density[22,23] and decrease in anisotropy[23,24] during H-assisted homoepitaxy and hydrogen coverage dependence of the growth behavior of silicon[25] and germanium[26] overlayers. The H/Si(100) system displays many unique properties, such as sticking probabilities that are greater than expected for Langmuirian adsorption,[1] first-order thermal desorption kinetics,[2,3] and Eley–Rideal (ER) abstraction by atomic hydrogen from the gas phase.[4] Despite the efficient abstraction, a high degree of passivation of the Si(100) surface can be achieved by exposure to atomic hydrogen due to the existence of ''reservoir'' adsorption sites[4,5] that help maintain a finite sticking probability at high coverages. Once the existence of dihydride and monohydride species on Si(100) was established,[6] a generally accepted view of hydrogen phases on Si(100) was developed. It is known that H/Si(100) has a 3×1 structure at 400 K consisting of alternating monohydride and dihydride units[7,8] with a coverage of 1.33 ML and a 2×1 monohydride structure at 600 K with a coverage of 1 ML.[9] At lower temperatures, 1.5 ML (Ref. 10) at 373 K and 1.6 ML (Ref. 3) at 110 K deuterium coverages were measured, although the (1×1) phase to which they correspond is not well defined.[7,8]

Currently, no measurements of H adsorption kinetics on Si(100) exist for a continuous range of temperatures between 325 and 750 K. This paper presents measurements of H atom adsorption dynamics and steady-state saturation values on Si(100) in this temperature range. The data reveal a continuous change in the hydrogen atom saturation coverage, in contrast with a widely accepted view of the Si(100)/H surface as having three fixed coverage states within certain temperature windows. The adsorption dynamics for temperatures between 500 and 650 K is interpreted by means of a kinetic model that includes adsorption, abstraction, and migration of H atoms between two types of adsorption sites. As different from other models, this model takes into account a finite migration time and permits a nonzero population of the secondary adsorption sites, permitting the total surface coverage to exceed unity. The trend in saturation values is explained using one temperature-dependent constant—the rate of hops from precursor to primary adsorption sites. The final filling of the dangling bonds occurs after the hydrogen source is shut off, when the Eley–Rideal abstraction is absent, but migration from secondary to primary sites continues. Coverages higher than 1 ML are obtained as a result of residual population of secondary sites. The steady-state population of primary sites after the adsorption is unity for all temperatures from 500 to 650 K, while the population of secondary sites decreases with temperature due to enhanced diffusion to the primary sites.

II. EXPERIMENT

A. Setup

A detailed description of the basic experimental setup has been given elsewhere.[27] Briefly, a time-of-flight (TOF) analysis of scattered and recoiled particles was performed in a stainless steel ultrahigh vacuum chamber with a base pressure $\sim 2\times10^{-10}$ Torr. A primary 4 keV Ne^+ ion beam pulsed at a rate of 30 kHz with a 50 ns pulse width and a ~ 0.1 nA/cm^2 average ion flux was used for scattering from a

[a]Permanent address: A. F. Ioffe Physical-Technical Institute, Russian Academy of Sciences, St. Petersburg 194021 Russia.
[b]Author to whom correspondence should be addressed.

Si(100) target. The scattered and recoiled particles were velocity analyzed through a 90 cm-long time-of-flight drift region and detected by a channeltron multiplier. TOF analysis allowed detection of both neutral particles and ions with high efficiency. The system contains LEED optics and a sputter ion gun for sample cleaning. The channeltron detector could be rotated in the scattering plane (the plane formed by the sample normal and beam line), allowing a continuous change in the scattering angle. The samples were mounted on a conventional manipulator that provides reproducible rotation in both azimuthal δ and incident α angles to within $\pm 1°$. The sample temperature was measured by a calibrated infrared pyrometer and a thermocouple attached to the back of the sample.

B. Sample preparation

The 2×2 cm Si samples were cut from a 0.005–0.02 Ω cm *p*-type silicon wafer and mounted on a two-axis goniometer for polar and azimuthal angle rotations with respect to the primary ion beam. Annealing was accomplished by electron bombardment or radiative heating from behind the sample. Before each adsorption run, the sample was repeatedly flushed to 1500 K for 10–15 s and gradually cooled to 800 K with the ambient pressure remaining at 7×10^{-10} Torr or lower throughout the cleaning cycle. The surface quality was monitored by LEED and the cleaning procedure was repeated until a sharp (2×1) two-domain LEED pattern characteristic of the clean Si(100) surface was observed. After several heating-cooling cycles, irreversible damage to the surface occurred due to etching by hydrogen at room temperature[8,11] and the sample had to be replaced. In order to avoid such damage, the sample was maintained at an elevated temperature between experiments. The clean surface quality was also checked by measuring the incident angle dependence of the scattered Ne ion fraction, $Ne^+/(Ne^0+Ne^+)$.

The Si(100)–2×1-H surface was prepared by cooling the sample to 600 K and dosing it until saturation with atomic hydrogen (molecular hydrogen pressure was 2×10^{-7} Torr). Atomic hydrogen was produced by dissociation of H_2 at a hot spiral W filament placed ~10 cm in front of the sample and heated to 2100 K. Adsorptions at other temperatures were performed in a similar manner. In order to prevent contamination of the highly reactive Si surface with the ambient gas, hydrogen exposure was carried out immediately after the sample was cooled down to the required temperature.

III. RESULTS

In order to measure the relative amount of adsorbed hydrogen, the ratio of H atoms recoiled from the surface to scattered primary Ne particles was monitored as a function of hydrogen exposure. Since TOF-SARS has equal detection efficiencies for ions and neutrals in this energy range, the signal from recoiled hydrogen does not depend on the chemical environment at different adsorption sites. The only factors that should be taken into account when comparing the recoiling intensities from different sites are scattering/recoiling cross sections and possible shadowing/blocking of trajectories. Our simulations have shown that for H atoms adsorbed above the first layer of the substrate, the predominant mechanism leading to forward recoiling of hydrogen is a single direct encounter with the incoming Ne projectile, independent of the atom position in the surface unit cell. Therefore the scattering/recoiling cross sections are constant and the shadowing/blocking of trajectories are nonexistent under these conditions. The hydrogen position near the top layer Si atoms, indicated by simulations[5] as a candidate for a secondary adsorption site, was also tested. In general, recoiling intensities from this site and the primary monohydride site differed; however, for the specific azimuth of 15° off the main channeling surface direction used in experiment, these two intensities were equal.

TABLE I. Initial uptake slopes for H adsorption on Si(100) at different surface temperatures.

T_S (K)	323	553	583	683	728
$r_1\times10^3$, ML/s	4.3±0.2	4.3±0.5	4.8±0.8	4.6±0.4	4.8±0.4

The isothermal hydrogen adsorption at different temperatures with constant atomic H flux was carried out in a series of experiments. All data were normalized to the reference signal from a 1 ML monohydride obtained from a saturated surface at $T_S=600$ K.

Uptake slopes at the initial stages of adsorption at different temperatures are presented in Table I, indicating constancy of the initial sticking coefficient over a wide range of temperatures. Assuming a unity sticking probability, these slopes may be used to estimate the atomic hydrogen flux F_H. The value obtained for a H_2 pressure of 2×10^{-7} Torr was $F_H=3.1\times10^{12}\,s^{-1}\,cm^{-2}$.

Figure 1 shows plots of the measured hydrogen coverage versus the exposure time for three substrate temperatures, $T_S=423$, 638, and 743 K. In all cases, the H_2 source was turned off after saturation was achieved and the hydrogen

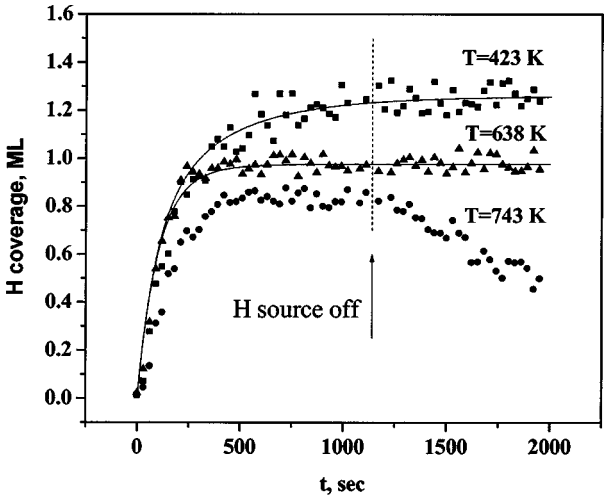

FIG. 1. Hydrogen adsorption dynamics on Si(100) at 423 K (squares), 663 K (triangles), and 743 K (circles). The hydrogen source was turned off at $t=1140$ s. Solid lines show fits by solutions to Eqs. (3) and (4) with $R_1=1$, $R_2=0.48$, $A_1=0.52$, $A_2=0.104$, and temperature-dependent κ.

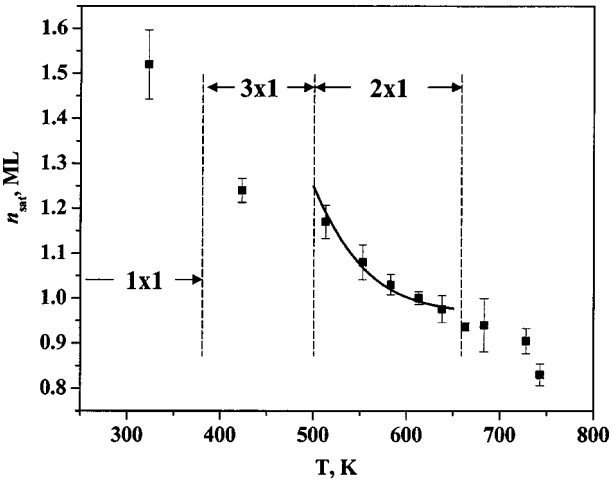

FIG. 2. Experimental measurements (squares) of H saturation coverage as a function of substrate temperature. Three regions corresponding to (1×1), (3×1), and (2×1) phases of H on Si(100) are shown. The solid line is the stationary solution $n_{sat}=n_{1sat}+n_{2sat}$ to Eqs. (3) with migration constant κ as a temperature-dependent parameter following the Arrhenius law.

surface population was monitored for some time after the shut-off. For $T_S=743$ K, as well as for all temperatures higher than 680 K (not shown), a decrease in coverage after the H atom shut-off was observed and attributed to thermal desorption from the main monohydride sites. For $T_S=423$ and 670 K, no change in hydrogen coverage was detected after the H atom shut-off, but the saturation values were different. The saturation values for various substrate temperatures from the interval $T_S=323-743$ K are plotted in Fig. 2, from which a continuous decrease of final H coverage with increasing temperature is observed. Figure 2 can be separated into regions corresponding to coverages characteristic of the three phases existing on the H-saturated Si(100) surface.[7–9] The main 1 ML (2×1) monohydride phase, the 1.33 ML (3×1) phase, and a disordered 1.5–2 ML (1×1) phase can be assigned to temperatures centered around 600, 400, and 300 K, respectively. Contrary to the accepted view that the coverage associated with the (2×1) monohydride phase is constant and equal to 1 ML, Fig. 2 shows that the saturation coverage inside the (2×1) region (500–650 K) actually varies with temperature. There is no thermal desorption in this temperature range and variations cannot be caused by change in the thermal desorption rate, as it is in the case[12] for $T_S>650$ K. In the following section we propose a new mechanism for this coverage variation. A kinetic model with two types of adsorption sites describing H adsorption on Si(100) is presented and coverage variations are interpreted from this model.

IV. ADSORPTION MODEL

In a manner similar to the description of monohydride adsorption[1] at a fixed temperature of 600 K, we investigate the possibility of kinetic equilibrium for a range of temperatures, $T_S=500-650$ K, in which the H atom coverage may exceed 1 ML. According to measurements of removal rates of adsorbed H by D atoms[4] and molecular dynamics simulations[5] of H on Si(100), an efficient Eley–Rideal abstraction of chemisorbed atoms by gaseous H atoms takes place during the adsorption phase. Inclusion of abstraction leads to the appearance of an additional negative term (an) in the kinematic adsorption equation as

$$\frac{dn}{dt}=r(1-n)-an. \tag{1}$$

Here, a is the abstraction rate, r is the adsorption rate, and n is the fractional H atom coverage. The saturation coverage value is obtained from Eq. (1) as

$$n_{sat}=\frac{r}{a+r}. \tag{2}$$

Rates of the Eley–Rideal abstraction were found to be comparable with the rate of the primary adsorption reaction.[1,3,4] For example,[4] for $a\sim 0.36r$, Eq. (2) yields $n_{sat}\sim 0.74$, indicating that the complete passivation by hydrogen is impossible. In order to reconcile the Eley–Rideal abstraction with observations of a highly ordered monohydride phase with coverage close to 1 ML at 600 K,[8] it has been suggested[4,5] that additional ''reservoir'' hydrogen adsorption sites supply extra hydrogen to primary monohydride sites in order to offset the high abstraction rate. A number of models featuring secondary adsorption sites that assist in filling of primary sites have been proposed.[1,12] These make use of the Kisliuk model[28] by applying it to kinetic equations. Such an extension requires that the time it takes for a physisorbed particle to chemisorb is very short. These models do not contain any temperature-dependent parameters, and are therefore only applicable for fixed temperatures, e.g., monohydride at 600 K. In contrast to those models, the two main assumptions of the current model are: (1) the migration rate between secondary and primary sites depends on the surface temperature and (2) the migration rate cannot be considered instantaneous for all temperatures; for temperatures below 600 K it becomes comparable with the rates of adsorption and abstraction. The change of migration constant with temperature leads to redistribution of atoms between primary and secondary sites and, due to different abstraction rates from these sites, will influence the saturation coverage. With the onset of competition between adsorption and abstraction on the one hand and migration on the other, the primary sites are no longer able to accommodate all of the hydrogen from reservoir sites, causing the latter to be partially filled. Their non-negligible population contributes to the total coverage and is responsible for coverages in excess of 1 ML at lower temperatures. Since the population of the secondary sites is no longer small, it must be explicitly included in the model.

The proposed relevant competing reactions that occur during the adsorption are shown schematically in Fig. 3. The primary chemisorption reaction occurring with rate r_1 is saturation of the dangling Si bond [Fig. 3(a)]. This reaction proceeds directly,[5] without a H atom going through any intermediate state. The state of occupancy of the second Si atom in the dimer is not taken into account in this case, although for some reactions, such as recombinative thermal desorption,[13–15] preferential pairing of hydrogens on silicon dimers may play a significant role. When the primary adsorption site is occupied, a second hydrogen atom is trapped into

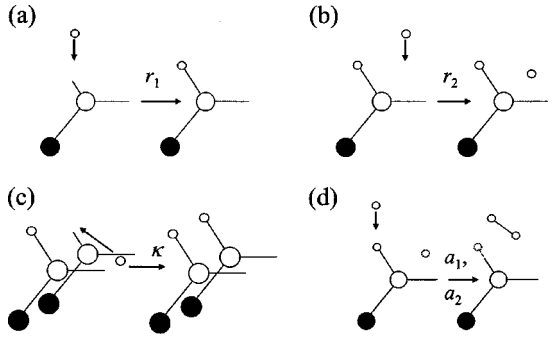

FIG. 3. Processes during H adsorption: (a) saturation of dangling bond, (b) adsorption to precursor state, (c) migration from precursor state to primary site, (d) Eley–Rideal abstraction. Small circles designate H atoms and light and dark circles designate first and second layer Si atoms, respectively.

a precursor (secondary) state [Fig. 3(b)] with rate r_2. Note that a secondary site is only filled when there is an adsorbed H atom at the primary site, since the potential well for the secondary site exists only in this case.[5] An atom in this state is highly mobile and can migrate to one of the neighboring unoccupied primary sites [Fig. 3(c)] with rate κ. Adsorbed atoms are assumed in the thermal equilibrium with the surface and κ is expected to exhibit an Arrhenius-type dependence on the surface temperature. Diffusion hops from filled primary sites (intradimer and intrarow) are not considered due to their high activation energies.[16] The Eley–Rideal abstraction [Fig. 3(d)] is possible from a singly or doubly occupied site with respective rates of a_1 and a_2. From the observed constancy of hydrogen coverage after the source shut-off (Fig. 1), it is concluded that desorption can proceed via abstraction by ambient atomic H only. If other types of desorption were present, such as thermally activated desorption or desorption by recombination of migrating H atoms, they would have been manifested by a drop in the coverage after the hydrogen shut-off.

Taking into account the above processes, the dynamic coupled equations describing hydrogen adsorption on Si(100) can be written as

$$\begin{aligned}\frac{dn_1}{dt} &= r_1(1-n_1) - a_1(n_1-n_2) + \kappa n_2(1-n_1),\\ \frac{dn_2}{dt} &= r_2(n_1-n_2) - a_2 n_2 - \kappa n_2(1-n_1),\end{aligned} \tag{3}$$

where n_1 and n_2 are the fractions of filled primary monohydride and precursor sites, respectively. The instantaneous time derivatives were obtained by multiplying the corresponding reaction rates by the fractions of sites available for a given transition. Adsorption and abstraction rates are proportional to the atomic hydrogen flux F_{H} as

$$\begin{aligned} r_i &= F_{\mathrm{H}} R_i \\ a_i &= F_{\mathrm{H}} A_i \end{aligned} \quad i = 1,2. \tag{4}$$

Here, R_i and A_i are the adsorption and abstraction probabilities and F_{H} is calculated with respect to one substrate atom. Steady-state solutions are obtained from Eqs. (3) by assuming $dn_1/dt = 0$, $dn_2/dt = 0$, and then solving the quadratic equation with respect to n_1 and n_2. In the high-temperature limit (large κ) the steady-state values for n_1 and n_2 are determined by reaction probabilities

$$n_{1\mathrm{sat}} = \frac{R_1}{R_1 + A_1 - R_2}; \quad n_{2\mathrm{sat}} = 0, \tag{5}$$

showing that in order for n_1 not to exceed unity, the abstraction probability from monohydride A_1 should be greater than the sticking probability R_2.

The reaction coefficients R_i and A_i were chosen to provide the best fit to the experimental results and at the same time be in agreement with the values that were reported in the literature. The sticking coefficient for atomic hydrogen on the clean surface R_1 is known to be temperature independent[1,3] and was assumed to be close to unity by many authors;[3,12,17] a value of 0.71 for $T_S = 500\,\mathrm{K}$ has been obtained from molecular dynamics calculations.[5] Our own measurements of initial slopes (Table I) for temperatures between 350 and 700 K confirm the independence of the initial adsorption rate r_1 on the temperature for coverages from 0 to 0.8 ML, in agreement with the fact that the primary adsorption reaction has no energy barrier. For the monohydride surface, both the sticking and abstraction probabilities are high and the reflection probability is nearly zero. In addition, the abstraction probability A_1 is also temperature independent.[4] It is reasonable to assume a similar behavior for R_2 and A_2 with respect to temperature as R_1 and A_1. Thus, the migration constant κ is the only temperature-dependent parameter in Eqs. (3). The much slower desorption rate from silicon surfaces with higher hydride concentrations,[4] as compared to the pure monohydride surface, implicates the reduced effectiveness of Eley–Rideal abstraction from the doubly occupied sites, or $A_2 < A_1$ in terms of abstraction probabilities. This constrictive, unexpected result was experimentally confirmed[4] by observing a decrease in the abstraction rate when the initial coverage increased from 1 to 1.25 ML. This may be related to the shape of the potential surface around the adsorbed hydrogen atoms. Since the migration rate from secondary to primary sites increases with temperature, the total coverage will decrease due to the greater abstraction rate from primary sites.

The following values were used in fitting experimental curves with solutions to Eqs. (3): $A_2 = 0.2\,A_1$, R_1 was taken to be unity, and reflection from the monohydride sites was neglected by assuming $R_2 = 0.48$ and $A_1 = 0.52$. The migration parameter κ was found for measured adsorption curves from the range $T_S = 325$–$650\,\mathrm{K}$ using their saturation coverages and steady-state solutions of Eqs. (3). The solid lines in Fig. 1 demonstrate fits of the two of the experimental curves by solutions to Eqs. (3) with previously determined constants κ. The third curve corresponding to $T_S = 743\,\mathrm{K}$ is given as an illustration of the monohydride thermal desorption. Figure 4 shows an Arrhenius plot for the migration constant and a linear fit that yields an activation energy E_A. From the slope of the plot, $E_A = 0.71\,\mathrm{eV}$. Once E_A and the intercept are known, the steady-state $n_{1\mathrm{sat}}(T)$ and $n_{2\mathrm{sat}}(T)$ can be calculated for any temperature T. The solid line in Fig. 2 shows $n_{\mathrm{sat}}(T) = n_{1\mathrm{sat}}(T) + n_{2\mathrm{sat}}(T)$ for $T_S = 500$–$650\,\mathrm{K}$ obtained by substituting $\kappa(T)$ into Eqs. (3). The agreement is good inside

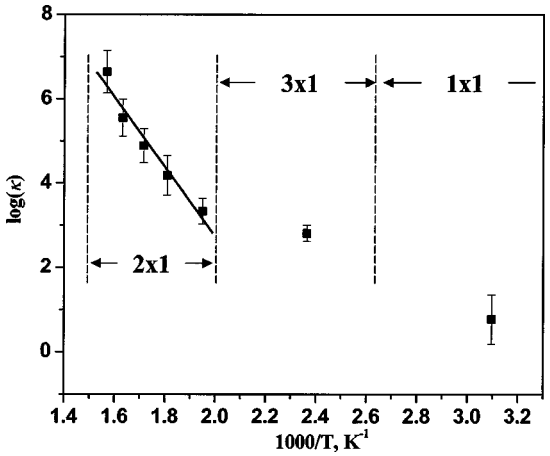

FIG. 4. Arrhenius plot of the migration constant κ from Eqs. (3) for $T_S = 500-650$ K. Squares, values of κ obtained by best fit of the experimental adsorption curves at different temperatures. The three regions showing different phases of H on Si(100) are the same as in Fig. 2.

this range; at the same time, an abrupt change in experimental n_{sat} for $T_S < 500$ K coinciding with the start of formation of the 3×1 phase is observed. The divergence for $T_S > 680$ K is associated with the onset of thermal monohydride desorption, which has been extensively studied[2,3,13,18] and is not the subject of the current work. It is possible to extend this model by adding terms describing first-order thermal desorption to the right-hand side of Eqs. (3).

Figure 5 shows the solutions to Eqs. (3) for the intermediate temperature $T_S = 500$ K. It follows that after the hydrogen source is shut off, there is a redistribution of adsorbed atoms between primary and precursor sites with the total population n_{sat} remaining unchanged. The characteristic time of this process is found from Eqs. (3) as $\tau = \kappa(n_{\mathrm{sat}} - 1)$.

V. DISCUSSION

Although the nature of the secondary site bonding with the surface and its exact position cannot be determined from the proposed empirical model, a comparison between different adsorption sites based on the migration activation energy can be made. In this connection, it is interesting to address

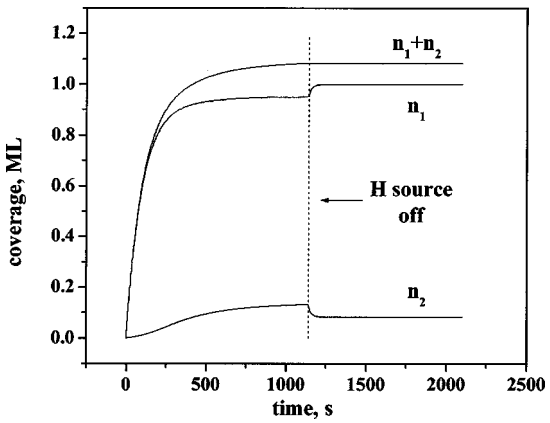

FIG. 5. Solutions to Eqs. (3) describing the process of H adsorption at $T_S = 500$ K. The populations of primary and precursor sites are n_1 and n_2, respectively. The total population is $n = n_1 + n_2$.

the relation between the adsorption site for the second H atom from a dihydride unit[7] and a secondary adsorption site existing above the line connecting the dimer atoms suggested as a precursor state.[21] The geometric positions of both sites are very close, and if these sites are in fact identical, our model should be able to describe the adsorption for all temperatures below 650 K. The observed deviation of the measured coverage from our model for $T_S < 500$ K, when the onset of filling of the dihydride units occurs, suggests that these two types of adsorption sites are different. Thus, our model indirectly supports the results of simulations,[5] where the potential minimum that is a candidate for the secondary adsorption site is located at approximately the same height as the first-layer Si atoms. Moreover, the activation energy for migration $E_A = 0.71$ eV obtained here is comparable with the depth of 0.8 eV for the above mentioned potential well[5] and higher than the energy barrier of 0.5 eV for migration of hydrogen along the dimer rows between precursor states located above the dimer pairs.[21]

The model presented herein explains variations in hydrogen atom coverage on Si(100) with temperature as a result of changing rates of reactions occurring at the surface. A thermodynamic equilibrium between the various states of hydrogen atoms on the surface,[10] when the ratios of the fractions of atoms in various states depend on the temperature according to the vibrational partition functions of these states, leads to similar conclusions. A crucial test that may give preference to one of the models lies in observing the effect of the change in flux of the impinging hydrogen. It follows from Eqs. (3) and (4) that the adsorption time and saturation coverage depend not only on the temperature, but also on the atomic hydrogen flux F_{H}. In Eqs. (3), the flux variation $F_{\mathrm{H}} \rightarrow \alpha F_{\mathrm{H}}$ is equivalent to transformations $t \rightarrow \alpha t$ and $\kappa \rightarrow \kappa \alpha^{-1}$ that effectively decrease the transition times and migration constant by the factor of α. This decrease leads to an increase in saturation coverage, while in the case of thermodynamic equilibrium the state populations should remain constant. The effect should be more pronounced for lower temperatures, since for temperatures close to 600 K the diffusion rate is much higher than the adsorption rates.

Other models have used sticking probabilities calculated by Kisliuk[28] to determine the instantaneous adsorption rate.[1,12] This application of the Kisliuk adsorption model is only valid if there is no appreciable change in coverage during the time τ it takes a physisorbed atom to attach to a chemisorption site or to be desorbed, i.e., $|dn/dt|\tau \ll 1$. This assumption neglects the population of secondary adsorption sites at any moment, but at the same time makes the model valid only for coverages less than or equal to unity. The Kisliuk model corresponds to the case of a large migration constant κ in the model presented here.

There is an ongoing discussion as to the exact mechanisms of hydrogen adsorption and abstraction on Si(100) and the nature of the secondary adsorption sites. Although direct interaction with primary sites seems to be the most likely mechanism supported by molecular dynamics simulations,[5] other data are consistent with adsorption and abstraction via a ''hot-precursor'' state.[1] The desorption by impinging hydrogen may be occurring not through a direct Eley–Rideal

(ER) abstraction,[4] but via a more complicated ER-type reaction,[19] or a ''hot-complex'' mechanism.[20] Taking into account these new mechanisms would necessarily lead to changes in the model and may yield slightly different results.

VI. SUMMARY

TOF-SARS measurements of isothermal H adsorption on Si(100) for a continuous range of temperatures $T_S = 325-750\,\mathrm{K}$ have been performed for the first time. The saturation coverage was found to monotonically decrease with temperature from ~1.5 to 1 ML. A kinetic model describing competing processes of adsorption, abstraction, and migration between two types of adsorption sites was developed to explain the observed dependencies in the range 500–650 K. In this model, the significant concentration of hydrogen atoms occupying secondary precursor sites acts as a reservoir for maintaining a finite sticking probability at high coverages. The temperature dependence of the coverage is interpreted by using a single temperature-dependent parameter, namely the rate of migration from secondary sites to primary monohydride sites. This rate cannot be considered instantaneous for temperatures below 600 K, leading to a decrease in the flow of hydrogen from reservoir sites to primary sites. Coverages higher than 1 ML are obtained as a result of residual population of the secondary sites. The final filling of the dangling bonds occurs after the hydrogen source shut-off, in the absence of the Eley–Rideal abstraction, with a characteristic time of $\kappa(n_{\mathrm{sat}}-1)$. The activation energy obtained for the migration constant $E_A = 0.71\,\mathrm{eV}$ is in good agreement with the reported energy barrier for chemisorption of a trapped state hydrogen into a monohydride state.

ACKNOWLEDGMENTS

This material is based on work supported by the National Science Foundation under Grant No. 0303708 and the R. A. Welch Foundation under Grant No. E-656.

[1] W. Widdra, S. I. Yi, R. Maboudian, G. A. D. Briggs, and W. H. Weinberg, Phys. Rev. Lett. **74**, 2074 (1995).
[2] K. Sinniah, M. G. Sherman, L. B. Lewis, W. H. Weinberg, J. T. Yates, Jr., and K. C. Janda, Phys. Rev. Lett. **62**, 567 (1989).
[3] K. Sinniah, M. G. Sherman, L. B. Lewis, W. H. Weinberg, J. T. Yates, Jr., and K. C. Janda, J. Chem. Phys. **92**, 5700 (1990).
[4] D. D. Koleske, S. M. Gates, and B. Jackson, J. Chem. Phys. **101**, 3301 (1994).
[5] U. Hansen and P. Vogl, Phys. Rev. B **57**, 13295 (1998).
[6] T. Sakurai and H. D. Hagstrum, Phys. Rev. B **14**, 1593 (1975).
[7] John J. Boland, Phys. Rev. Lett. **65**, 3325 (1990).
[8] John J. Boland, Surf. Sci. **261**, 17 (1992).
[9] H. N. Waltenburg and J. T. Yates, Jr., Chem. Rev. (Washington, D.C.) **95**, 1589 (1995); K. W. Kolasinski, Int. J. Mod. Phys. B **9**, 2753 (1995); K. Oura, V. G. Lifshits, A. A. Saranin, A. V. Zotov, and M. Katayama, Surf. Sci. Rep. **35**, 1 (1999).
[10] M. C. Flowers, N. B. H. Jonathan, A. Morris, and S. Wright, Surf. Sci. **396**, 227 (1998).
[11] Y. Wei, L. Li, and I. S. T. Tsong, Appl. Phys. Lett. **66**, 1818 (1995).
[12] Y.-J. Zheng, J. R. Engstrom, J. Zhang, A. Schellinger, and B. A. Joyce, Surf. Sci. **470**, 131 (2000).
[13] M. P. D'Evelyn, Y. L. Yang, and L. F. Sutcu, J. Chem. Phys. **96**, 852 (1992).
[14] John J. Boland, Phys. Rev. Lett. **67**, 1539 (1991).
[15] John J. Boland, J. Vac. Sci. Technol. A **10**, 2458 (1992).
[16] E. Hill, B. Freelon, and E. Ganz, Phys. Rev. B **60**, 15896 (1999).
[17] S. K. Jo, J. H. Kang, X.-M. Yan, J. M. White, J. G. Ekerdt, J. W. Keto, and J. Lee, Phys. Rev. Lett. **85**, 2144 (2000).
[18] D.-S. Lin and R.-P. Chen, Phys. Rev. B **60**, R8461 (1999).
[19] A. Kubo, Y. Ishii, and M. Kitajima, J. Chem. Phys. **117**, 11336 (2002).
[20] E. Hayakawa, F. Khanom, T. Yoshifuku, S. Shimokawa, A. Namiki, and T. Ando, Phys. Rev. B **65**, 033405 (2002).
[21] E. S. Tok, J. R. Engstrom, and H. Chuan Kang, J. Chem. Phys. **118**, 3294 (2003).
[22] J. E. Vasek, Z. Zhang, C. T. Salling, and M. G. Lagally, Phys. Rev. B **51**, 17207 (1995).
[23] M. Fehrenbacher, J. Spitzmüller, U. Memmert, H. Rauscher, and R. J. Behm, J. Vac. Sci. Technol. A **14**, 1499 (1996).
[24] D.-S. Lin, E. S. Hirschorn, T.-C. Chiang, R. Tsu, D. Lubben, and J. E. Greene, Phys. Rev. B **45**, 3494 (1992).
[25] M. Copel and R. M. Tromp, Phys. Rev. Lett. **72**, 1236 (1994).
[26] A. Sakai and T. Tatsumi, Appl. Phys. Lett. **64**, 52 (1994).
[27] O. Grizzi, M. Shi, H. Bu, and J. W. Rabalais, Rev. Sci. Instrum. **61**, 740 (1990).
[28] P. Kisliuk, J. Phys. Chem. Solids **3**, 95 (1957).